

# Mechanistic Studies of Photochemical Silylene Extrusion from 2,2-Diphenylhexamethyltrisilane

Takashi Miyazawa,<sup>‡,§</sup> Shin-ya Koshihara,<sup>‡,§</sup> Chengyou Liu,<sup>‡</sup> Hideki Sakurai,<sup>†,||</sup> and Mitsuo Kira<sup>\*,†,‡</sup>

Contribution from the Department of Chemistry, Graduate School of Science, Tohoku University, Aoba-ku, Sendai 980-8578, Japan, and Photodynamics Research Center, the Institute of Physical and Chemical Research, (RIKEN), 19-1399, Koeji, Nagamachi, Aoba-ku, Sendai 980-0952, Japan

Received September 21, 1998

**Abstract:** Photophysics and photochemistry of 2,2-diphenylhexamethyltrisilane (**1**) was investigated in detail. Diphenyltrisilane **1** showed an intense fluorescence band assignable to the intramolecular charge-transfer (ICT) band in a polar solvent. Whereas silylene extrusion and 1,3-silyl migration were the major photoreactions of **1** in a nonpolar solvent, solvolytic cleavage of the Si–Si bond occurred significantly in an ethanol–hexane mixture; the ICT state is responsible for the latter reaction. Solvent and temperature dependence of the product distribution has indicated that both the silylene extrusion and the 1,3-silyl migration take place from the nonpolar but electronically different excited states of **1**. On the basis of the photoreactions of **1** using a nonresonant two-photon (N RTP) excitation method, it is suggested that the silylene extrusion occurs via the <sup>1</sup>L<sub>a</sub> state of **1** as a silyl-substituted benzene.

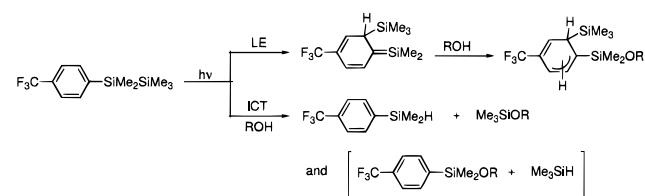
## Introduction

Aryllogosilanes constitute a fascinating class of molecular systems, exhibiting unique photophysical and photochemical properties due to hyperconjugation between aromatic  $\pi$  orbitals and high-lying Si–Si  $\sigma$  orbitals,<sup>1</sup> low ionization potentials,<sup>2</sup> remarkable red-shift of the <sup>1</sup>L<sub>a</sub> bands<sup>3</sup> and their stereoelectronic effects,<sup>4</sup> and dual fluorescence in aryltrisilanes.<sup>5,6</sup> With close similarity to so-called TICT molecules like *p*-dimethylaminobenzonitrile,<sup>7</sup> aryltrisilanes in solution show intramolecular charge-transfer (ICT) emission bands, where the disilanyl group and the aryl  $\pi$  system serve as an electron donor and an acceptor,

respectively, in addition to a regular emission band from an aromatic  $\pi\pi^*$  (LE, locally excited) state; we have revealed recently that jet-cooled *p*-cyanophenylpentamethyldisilane shows the ICT emission even in an isolated molecular condition.<sup>6d</sup>

Much attention has been focused also on the photochemical reactions and their mechanistic aspects of aryltrisilanes,<sup>1</sup> since they generate interesting reactive intermediates such as silylenes, silenes, and silyl radicals. In our previous study<sup>6c</sup> of mechanisms of photoreactions of *p*-trifluoromethylphenylpentamethyldisilane in the presence of alcohols, we have revealed that the LE and the ICT states participate in the photoreactions; 1,3-silyl migration to give a silatriene intermediate, which is the most predominant pathway in a nonpolar solvent, occurs via the LE state, while significant direct solvolysis of the ICT state takes place in an alcoholic solvent (Scheme 1).

## Scheme 1



Whereas it has been well-known that photolysis of 2-aryl-trisilanes provides a useful method for generation of the corresponding 2-arylsilylenes,<sup>1,8–10</sup> the 1,3-silyl migration to give the corresponding silatriene occurs competitively, similar to the photolysis of aryltrisilanes (Scheme 2). No detailed

(6) (a) Sakurai, H.; Sugiyama, H.; Kira, M. *J. Phys. Chem.* **1990**, *94*, 1837. (b) Kira, M.; Miyazawa, M.; Mikami, N.; Sakurai, H. *Organometallics* **1991**, *10*, 3793. (c) Kira, M.; Miyazawa, T.; Sugiyama, H.; Yamaguchi, M.; Sakurai, H. *J. Am. Chem. Soc.* **1993**, *115*, 3116. (d) Tajima, Y.; Ishikawa, H.; Miyazawa, T.; Kira, M.; Mikami, N. *J. Am. Chem. Soc.* **1997**, *119*, 7400.

(7) For recent reviews, see: (a) Rettig, W. *Angew. Chem., Int. Ed. Engl.* **1986**, *25*, 971. (b) Bhattacharyya, K.; Chowdhury, M. *Chem. Rev.* **1993**, *93*, 507.

<sup>†</sup> Tohoku University.

<sup>‡</sup> The Institute of Physical and Chemical Research.

<sup>§</sup> Present address: Kanagawa Academy of Science and Technology, KSP East, 3-2-1 Sakado, Takatsu-ku, Kawasaki-shi, Kanagawa, 213-0012, Japan.

<sup>||</sup> Present address: Department of Industrial Chemistry, Faculty of Science and Technology, Science University of Tokyo, Noda, Chiba 278-8510, Japan.

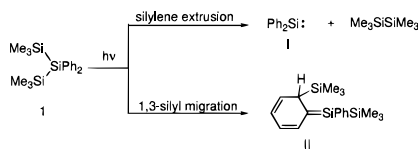
(1) For recent reviews, see: (a) Kira, M.; Miyazawa, T. In *The Chemistry of Organic Silicon Compounds*; Rappoport, Z., Apeloig, Y., Eds.; John Wiley: New York, 1998; Vol. 2, Chapter 22. (b) Brook, A. G. In *The Chemistry of Organic Silicon Compounds*; Rappoport, Z., Apeloig, Y., Eds.; John Wiley: New York, 1998; Vol. 2, Chapter 21. (c) Brook, A. G. In *The Chemistry of Organic Silicon Compounds*; Patai, S., Rappoport, Z., Eds.; John Wiley: New York, 1989; Chapter 15. (d) Steinmetz, *Chem. Rev.* **1995**, *95*, 1527. (e) Sakurai, H. *J. Organomet. Chem.* **1980**, *200*, 261. (f) Ishikawa, M.; Kumada, M. *Adv. Organomet. Chem.* **1981**, *19*, 51.

(2) (a) Bock, H.; Alt, H. *J. Am. Chem. Soc.* **1970**, *92*, 1569. (b) Pitt, C. G.; Carey, R. N.; Toren, E. C., Jr. *J. Am. Chem. Soc.* **1972**, *94*, 3806. (c) Sakurai, H.; Kira, M. *J. Am. Chem. Soc.* **1974**, *96*, 791. (d) Sakurai, H.; Kira, M. *J. Am. Chem. Soc.* **1975**, *97*, 4879. (e) Pitt, C. G.; Bock, H. *J. Chem. Soc., Chem. Commun.* **1972**, 28.

(3) Sakurai, H.; Kumada, M. *Bull. Chem. Soc. Jpn.* **1964**, *37*, 1894. (b) Gilman, H.; Atwell, W. H.; Schwebke, G. L. *J. Organomet. Chem.* **1964**, *2*, 369. (c) Hague, D. N.; Prince, R. H. *Chem. Ind. (London)* **1964**, 1492.

(4) Sakurai, H.; Tasaka, S.; Kira, M. *J. Am. Chem. Soc.* **1972**, *94*, 3806. (5) (a) Shizuka, H.; Obuchi, M.; Ishikawa, M.; Kumada, M. *J. Chem. Soc., Chem. Commun.* **1981**, 405. (b) Shizuka, H.; Sato, Y.; Ishikawa, M.; Kumada, M. *J. Chem. Soc., Chem. Commun.* **1982**, 439. (c) Shizuka, M.; Sato, Y.; Ueki, Y.; Ishikawa, M.; Kumada, M. *J. Chem. Soc. Faraday Trans. 1* **1984**, *80*, 341. (d) Shizuka, H.; Obuchi, M.; Ishikawa, M.; Kumada, M. *J. Chem. Soc., Faraday Trans. 1* **1984**, *80*, 383. (e) Hiratsuka, H. Mori, Y.; Ishikawa, M.; Okazaki, K.; Shizuka, H. *J. Chem. Soc., Faraday Trans. 2* **1984**, *81*, 1665. (f) Shizuka, H. *Pure Appl. Chem.* **1993**, *65*, 1635.

## Scheme 2



mechanistic study of the photoreactions of 2-aryltrisilanes has been reported, whereas the manner in which the ICT state participates in the photoreactions is an interesting issue. In this paper, we have investigated in detail the photophysics and photochemistry of 2,2-diphenylhexamethyltrisilane (**1**) and revealed that, while the two types of the photoreactions, silylene extrusion and 1,3-silyl migration, occur from nonpolar excited states of **1**, the electronic natures of the excited states are different from each other. On the basis of the photoreactions of **1** using a nonresonant two-photon (NRTP) excitation method,<sup>11,12</sup> it is suggested that the excited state responsible for the silylene extrusion is the two-photon allowed excited state.

## Results and Discussion

**ICT Fluorescence Spectra.** As mentioned above, phenyl-disilanes in solution show the characteristic ICT fluorescence, in addition to the nonpolar LE fluorescence. In a previous paper,<sup>6c</sup> we have taken the fact that the maximum wavelength and the quantum yield of the emission band increase with increasing concentration of dichloromethane in hexane, i.e. with increasing the solvent polarity, as the evidence for the ICT nature of the emission band in *p*-trifluoromethylphenylpentamethyldisilane. Diaryltrisilane **1** in hexane ( $5.59 \times 10^{-5}$  M) with a small amount of dichloromethane (1.0 M) showed an intense fluorescence band maximum at around 344 nm as shown in Figure 1; however, the emission is too weak to be observed in the absence of dichloromethane. The emission band red-shifted, and the quantum yield increased with increasing the concentration of dichloromethane as shown in Table 1, indicating the ICT nature of the emission. According to the discussion in the previous paper,<sup>6c</sup> we have tested whether the kinetic profile shown in Figure 2 is applicable, where  $k_f$  and  $k_f'$  are the fluorescence rate constants for nonpolar excited (NPE) and ICT states, respectively, and  $k_D$  and  $k_D'$  are the inherent rate constants for unimolecular deactivation of NPE and ICT states, respectively, while the reaction rates in the figure are not taken explicitly into consideration in dichloromethane. The rate constant for the formation of ICT from the NPE state,  $k_C$ , is assumed to be represented by a linear function of the concentration of a polar solvent ( $[S] = [\text{CH}_2\text{Cl}_2]$ , eq 1)<sup>13</sup>

$$k_C = k_{C0} + k_{C'}[S] \quad (1)$$

(8) (a) Ishikawa, M.; Kumada, M. *J. Organomet. Chem.* **1974**, *81*, C3. (b) Ishikawa, M.; Nakagawa, K.; Ishiguro, M.; Ohi, F.; Kumada, M. *J. Organomet. Chem.* **1978**, *152*, 155. (c) Ishikawa, M.; Nakagawa, K.; Ishiguro, M.; Ohi, F.; Kumada, M. *J. Organomet. Chem.* **1980**, *201*, 151.

(9) Inter alia: (a) Michalczyk, M. J.; Fink, M. J.; De Young, D. J.; Carlson, C. W.; Welsh, K. M.; West, R.; Michl, J. *Silicon, Germanium, Tin, Lead Compds.* **1986**, *9*, 75. (b) West, R. *Pure Appl. Chem.* **1984**, *56*, 163. (c) West, R.; Fink, M. J.; Michl, J. *Science* **1981**, *214*, 1343.

(10) (a) Kira, M.; Maruyama, T.; Sakurai, H. *Chem. Lett.* **1993**, 1345.

(11) Kira, M.; Miyazawa, T.; Koshihara, S.; Segawa, Y.; Sakurai, H. *Chem. Lett.* **1995**, 3.

(12) (a) Miyazawa, T.; Koshihara, S.; Segawa, Y.; Kira, M. *Chem. Lett.* **1995**, 217. (b) Miyazawa, T.; Liu, Z.; Liu, C.; Koshihara, S.; Kira, M. *Chem. Lett.* **1996**, 1023. (c) Miyazawa, T.; Liu, C.; Kira, M. *Chem. Lett.* **1997**, 459. (d) Miyazawa, T.; Liu, C.; Koshihara, S.; Kira, M. *Photochem. Photobiol.* **1997**, *66*, 566. (e) Miyazawa, T.; Saeki, T.; Liu, C.; Kira, M. *J. Am. Chem. Soc.* **1998**, *120*, 1084.

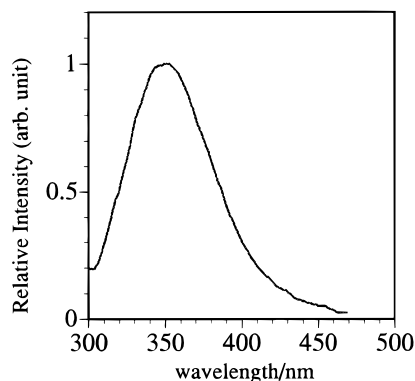


**Figure 1.** Fluorescence spectrum of **1** ( $1.45 \times 10^{-5}$  M) in the presence of dichloromethane (1 M) in hexane.

**Table 1.** Solvent Effects on the Fluorescence Band Maxima and the Quantum Yields of **1** in Dichloromethane–Hexane Mixtures<sup>a</sup>

$[\text{CH}_2\text{Cl}_2]/\text{M}^b$	$\lambda_{\text{max}}/\text{nm}$	$\Phi_{\text{rel}}$	$[\text{CH}_2\text{Cl}_2]/\text{M}^b$	$\lambda_{\text{max}}/\text{nm}$	$\Phi_{\text{rel}}$
1.0	344	1.0	7.7	361	6.0
1.4	346	1.1	10.9	362	7.3
2.9	347	2.2	12.3	363	11.0
4.6	358	3.3			

<sup>a</sup> Concentration of **1** in the mixed solvents and temperature was fixed to  $5.59 \times 10^{-5}$  M and  $22.5 \pm 0.5$  °C, respectively. <sup>b</sup> Molar concentration of dichloromethane in hexane.

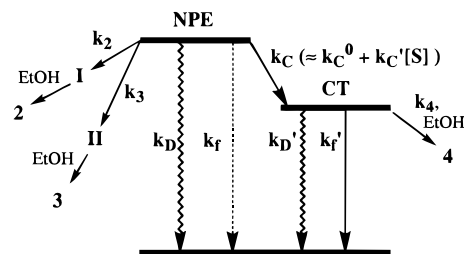


**Figure 2.** Kinetic profile for the photophysical and photochemical processes of **1** in a polar solvent.

In this situation, the relative quantum yields of the ICT fluorescence,  $\Phi_f^0/\Phi_f$ , where  $\Phi_f^0$  and  $\Phi_f$  are the ICT fluorescence quantum yields at the concentrations of dichloromethane of 1.0 M and  $[\text{CH}_2\text{Cl}_2]$  M, respectively, should fulfill the following equation (eq 2), where  $\tau = 1/(k_D + k_f + k_C^0)$ :

$$\frac{\Phi_f^0}{\Phi_f} = \frac{k_C^0 + k_{C'}}{1 + k_{C'}\tau} \cdot \frac{1 + k_{C'}\tau[S]}{k_C^0 + k_{C'}[S]} \quad (2)$$

If  $k_C^0 \ll k_{C'}[S]$ , then,  $\Phi_f^0/\Phi_f$  should show a linear dependence on  $[\text{CH}_2\text{Cl}_2]^{-1}$  (eq 3).

$$\frac{\Phi_f^0}{\Phi_f} = \frac{k_C^0 + k_{C'}}{1 + k_{C'}\tau} \left\{ \frac{1}{k_{C'}}[S] + \tau \right\} \quad (3)$$

Actually, a linear relationship between  $\Phi_f^0/\Phi_f$  and  $[\text{CH}_2\text{Cl}_2]^{-1}$  was found as shown in Figure 3 (slope, 1.49; intercept,  $-0.029$ ; correlation coefficient, 0.995),<sup>14</sup> indicating that the kinetic profile shown in Figure 2 is applicable to the photophysical processes of diphenyltrisilane **1**.

(13) Equation 1 does not mean the unimolecularity for S of the kinetics but should be taken as an approximate representation of the dependence of  $k_C$  on the solvent polarity as a function of power series of  $[S]$ .

(14) The ratio (intercept)/(slope) ( $= k_{C'}\tau$ ) is meaninglessly  $-0.02$ . On the basis of the very small value,  $k_{C'}\tau$  would be taken as almost 0 or  $< 10^{-2}$  within the accuracy of our experiments.

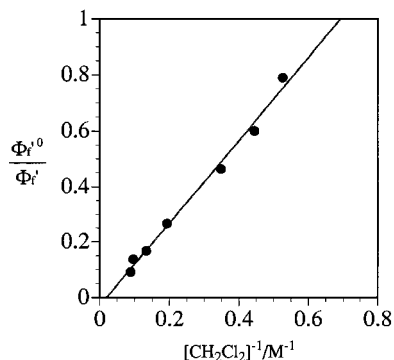


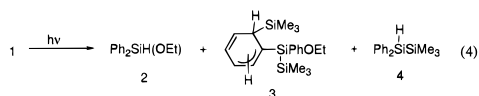
**Figure 3.** A plot of  $\Phi_f^0/\Phi_f$  vs  $[\text{CH}_2\text{Cl}_2]^{-1}$  during irradiation of **1** in  $\text{CH}_2\text{Cl}_2$ -hexane mixtures.

**Table 2.** Chemical Yields of the Photoproducts of **1** in Ethanol-Hexane Mixtures in Various Irradiation Conditions<sup>a</sup>

irradiation conditions		[EtOH]/M <sup>b</sup>	conv./%	products and yields/%		
light source	wavelength/nm			2	3	4
LP <sup>c</sup>	254	1.0	24	50	37	0
Nd:YAG <sup>d</sup>	266	1.0	30	53	30	0
Nd:YAG <sup>e</sup>	532	1.0	20	80	13	0
Ar(CW) <sup>f</sup>	514	1.0	0	0	0	0
LP <sup>c</sup>	254	13.6	35	24	21	16
Nd:YAG <sup>d</sup>	266	13.4	40	33	23	28
Nd:YAG <sup>e</sup>	532	13.4	48	37	6	46

<sup>a</sup> Irradiation was performed on ca.  $5 \times 10^{-3} - 1 \times 10^{-2}$  M of **1** in an ethanol-hexane mixture. <sup>b</sup> Molar concentration of ethanol in hexane. <sup>c</sup> A low-pressure Hg arc lamp (32 W). <sup>d</sup> The fourth harmonics of a pulsed Nd:YAG laser (5 ns, 10 Hz) with the intensity of 11 mJ/pulse. <sup>e</sup> The second harmonics of a pulsed Nd:YAG laser (6 ns, 10 Hz) with the intensity of 160 mJ/pulse. <sup>f</sup> A CW Ar<sup>+</sup> laser (2 W).

**Photoreactions of 1 in the Presence of Ethanol.** In accord with the previous results on the photoreactions of **1** in the presence of various trapping reagents,<sup>8</sup> photolysis of **1** ( $5.54 \times 10^{-3}$  M) using a 32-W low-pressure Hg arc lamp in the presence of ethanol (1.0 M) in hexane gave ethoxydiphenylsilane (**2**) and trimethylsilyl(1-ethoxy-1-phenyltrimethylsilyl)hexadienes (**3**) in 50 and 37% yields, respectively, with the consumption of 24% of **1**; **2** and **3** are ethanol adducts of diphenylsilylene (I) and a silyatriene intermediates (II) of the photoreactions of **1**, respectively (eq 4). On the other hand, a similar photolysis of **1** ( $5.54 \times 10^{-3}$  M) in a mixture of ethanol and hexane (concentration of EtOH, 13.6 M) showed suppression of the yields of **2** and **3** with the formation of a significant amount of 1,1,1-trimethyl-2,2-diphenyldisilane (**4**); the yields of **2**, **3**, and **4** are 24, 21, and 16%, respectively (Table 2). The results suggest that the silylene extrusion and the 1,3-silyl migration occur via NPE state(s) of **1**, while **4** would be derived from the direct solvolysis of the ICT excited state,<sup>15</sup> by analogy to the solvent effects of the photolysis of *p*-trifluoromethylphenylpentamethyldisilane.<sup>6c</sup> The results cannot differentiate however whether the two pathways occur via the same single excited state or via the two different NPE states.



**Solvent and Temperature Effects on Photochemical Silylene Extrusion from 1.** To examine the excited-state nature

(15) Expectedly, photolysis of **1** in ethanol-*d* gave deuterated hydrosilane **4-d**, where deuterium was incorporated almost quantitatively as Si-D.

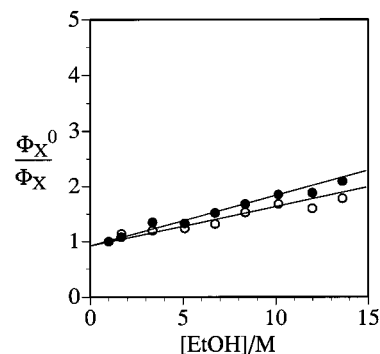


**Figure 4.** Plots of  $\Phi_2^0/\Phi_2$  and  $\Phi_3^0/\Phi_3$  vs  $[\text{EtOH}]$  during irradiation of **1** in EtOH-hexane mixtures: (●) silylene extrusion ( $x = 2$ ); (○) 1,3-silyl migration ( $x = 3$ ).

responsible for the silylene extrusion as well as for the 1,3-silyl migration, we have analyzed the dependence of quantum yields of the two photochemical pathways of **1** on the concentration of ethanol in hexane more in detail. Here again, the kinetic profile outlined in Figure 2 is applied, where  $k_2$ ,  $k_3$ , and  $k_4$  correspond to the reaction rate constants for the formations of I and II from NPE state(s)<sup>15</sup> and the direct ethanolysis of ICT state, respectively. Ethanol works as a trapping reagent of I and II, as a nucleophilic reagent of the ICT state, and as a cosolvent to increase the solvent polarity. On the basis of this kinetic profile, the dependence of the quantum yields and the relative yields on the concentration of ethanol will be represented by the following equations (eqs 5-7), where  $\Phi_2$  and  $\Phi_3$  are quantum yields for the silylene extrusion and the 1,3-silyl migration, respectively,  $\Phi_2^0$  and  $\Phi_3^0$  are those at the ethanol concentrations of 1.0 M, and  $k_s = k_2 + k_3 + k_D + k_f + k_C^0$ :

$$\Phi_2 = \frac{k_2}{k_s + k_C[\text{EtOH}]} \quad (5)$$

$$\Phi_3 = \frac{k_3}{k_s + k_C[\text{EtOH}]} \quad (6)$$

$$\frac{\Phi_2^0}{\Phi_2} = \frac{\Phi_3^0}{\Phi_3} = \frac{k_s + k_C[\text{EtOH}]}{k_s + k_C} \quad (7)$$

Thus,  $\Phi_2^0/\Phi_2$  and  $\Phi_3^0/\Phi_3$  should depend linearly on  $[\text{EtOH}]$  with the same slope and intercept. As shown in Figure 4, plots of  $\Phi_2^0/\Phi_2$  and  $\Phi_3^0/\Phi_3$  vs  $[\text{EtOH}]$  showed fairly good linear relationships with slopes of 0.082 and 0.058, and intercepts of 0.97 and 0.99, respectively (correlation coefficients, 0.966 and 0.987, respectively). Whereas the slopes of the two lines are slightly different, the results are in good accord with the idea that both the silylene extrusion and the 1,3-silyl migration do not occur from the polar ICT state but from the NPE state(s) of **1**. However, the results do not mean that the excited states responsible for the two pathways are identical, while the excited state responsible for the photochemical 1,3-silyl migration is acceptably assigned to the <sup>1</sup>L<sub>b</sub> state (Platt's notation) of **1**, on analogy of the photoreactions of *p*-trifluoromethylphenylpentamethyldisilane.<sup>6c</sup>

From the kinetic profile outlined in Figure 2,  $\Phi_4$  is represented by eq 8, where  $k_s' = k_D' + k_f'$ :

$$\Phi_4 = \frac{k_C^0 + k_C[\text{EtOH}]}{k_s + k_C[\text{EtOH}]} \cdot \frac{k_4[\text{EtOH}]}{k_s' + k_4[\text{EtOH}]} \quad (8)$$

Thus,  $\Phi_4/\Phi_2$  is proportional to  $[\text{EtOH}]^2$  as shown in eq 9,

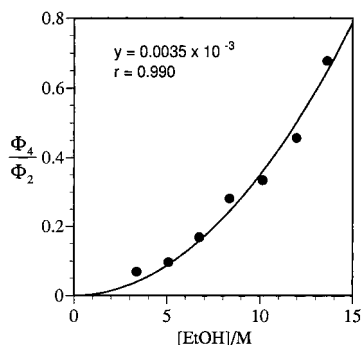


**Figure 5.** A plot of  $\Phi_4/\Phi_2$  vs [EtOH] during irradiation of **1** in EtOH–hexane mixtures.

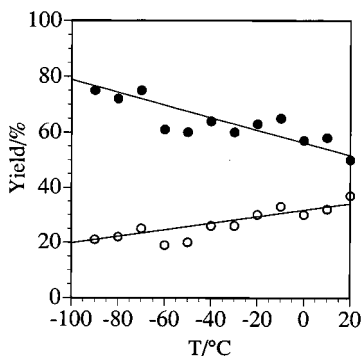


**Figure 6.** Plots of chemical yields of **2** (●) and **3** (○) vs temperatures (°C) during irradiation of **1** (ca.  $5 \times 10^{-3}$  M) in hexane in the presence of 1 M of ethanol.

if  $k_s' \gg k_4[\text{EtOH}]$  and  $k_C^0 \ll k_C'[\text{EtOH}]$ .

$$\frac{\Phi_4}{\Phi_2} = \frac{k_C^0 + k_C'[\text{EtOH}]}{k_2} \cdot \frac{k_4[\text{EtOH}]}{k_s' + k_4[\text{EtOH}]} = \frac{k_C k_4 [\text{EtOH}]^2}{k_2 k_s'} \quad (9)$$

A plot of  $\Phi_4/\Phi_2$  vs  $[\text{EtOH}]^2$  shown in Figure 5 is well fitted by the equation of  $\Phi_4/\Phi_2 = 3.5 \times 10^{-3} [\text{EtOH}]^2$  (correlation coefficient = 0.990).<sup>17</sup>

To gain further insight into the excited-state which participates in the silylene extrusion, temperature dependence of the yield of silylene extrusion relative to 1,3-silyl migration was investigated. Upon irradiation of **1** (ca.  $5 \times 10^{-3}$  M) in hexane in the presence of ethanol (1.0 M) using a low-pressure Hg arc lamp, **2** and **3** were obtained in 75 and 21% yields, respectively, at  $-90$  °C, while the yields of **2** and **3** at  $20$  °C were 50 and 37%, respectively (Table 2). As shown in Figure 6, the yield of **2** decreased but that of **3** increased with increasing temperature. Since the total yields of **2** and **3** were about 90% in the investigated temperature range, the temperature dependence of the yield ratio ( $Y_2/Y_3$ ) should not be caused by the difference of the efficiency of trapping of the intermediates by ethanol. Furthermore, the temperature dependence is not ascribed to the solvent viscosity effect. As shown in Table 3, even when the photolysis of **1** was carried out in a longer-chain alkane such as nonane ( $\eta = 0.716$ ) and tridecane ( $\eta = 1.88$ ) at  $20$  °C, similar  $Y_2/Y_3$  ratios to that in hexane ( $\eta = 0.313$ ) were obtained, while

(16) The NPE states are treated as a set in the subsequent discussion.

(17) As suggested by a reviewer, it is desirable to investigate a series of experiments in hexane/ $\text{CH}_2\text{Cl}_2$  mixtures at constant ethanol concentration, to elucidate the effects of solvent polarity on the importance of formations of **2** and **3** relative to that of **4**. However, the photolysis of **1** in such solvent systems gave a complex mixture including products from the photoreactions of **1** with dichloromethane. For photoreactions of an arylsilylene with a chloroalkane see: Sluggett, G. W.; Leigh, W. J. *Organometallics* **1994**, *13*, 1005.

**Table 3.** Relative Chemical Yields of **2** to **3** during Irradiation of **1** in Various Alkanes<sup>a</sup>

	hexane ( $20$ °C)	hexane ( $-90$ °C)	nonane ( $20$ °C)	tridecane ( $20$ °C)
<b>2/3</b>	1.4	3.0	1.6	1.7

<sup>a</sup> Irradiation was performed on a ca.  $5 \times 10^{-3}$  M solution of **1**.

the ratio increased up to 3.0 at  $-90$  °C in hexane ( $\eta = 1.014$ ).<sup>18</sup> A plot of  $\ln(Y_2/Y_3)$  vs.  $1/T$  gave a linear line, from which the value of 0.77 kcal/mol is estimated as the apparent difference of the activation enthalpies for the two pathways. The following are the possible explanations for the remarkable temperature dependence: (1) the two reactions occur from the same single excited state ( $^1L_b$ ) with small difference in the activation enthalpies for the two pathways, and (2) the two reactions occur from two different excited states ( $^1L_a$  and  $^1L_b$ ) with the enthalpy difference of 0.77 kcal/mol ( $270 \text{ cm}^{-1}$ ) but the two states are thermally equilibrated before the reactions take place. As discussed in the following section, the results of the nonresonant two-photon (NRTP) photochemistry of **1** eliminates, however, above two possibilities and suggests more effective silylene extrusion from the upper excited state ( $^1L_a$ ) than the lowest excited state ( $^1L_b$ ).

#### Nonresonant Two-Photon (NRTP) Photochemistry of **1**.

Recent advances in laser systems have allowed the application of an intense pulsed light to a molecule, which causes nonresonant two-photon (NRTP) absorption, i.e. simultaneous two-photon absorption, with significant efficiency in certain circumstances, as first predicted by Göppert-Mayer.<sup>19</sup> The NRTP absorption obeys the different selection rule from direct single-photon (SP) absorption; transition to the totally symmetric excited state from the singlet ground state via the NRTP excitation is allowed, while the transition via the SP excitation is forbidden. We have developed the NRTP excitation method as a novel and practical tool for modifying the photoreaction pathways in solution.<sup>11,12</sup> Typically, the NRTP excitation of *cis*- and *trans*-stilbene induces only *cis*–*trans* isomerization, while usual SP irradiation of the same molecules induces a cyclization giving 9,10-dihydrophenanthrene in addition to the *cis*–*trans* isomerization.<sup>12a</sup>

In a previous paper,<sup>11</sup> we have shown that the NRTP excitation of 2,2-diphenyltrisilane **1** using a 532-nm pulsed laser light induces the silylene extrusion and the 1,3-silyl migration with a quite different selectivity from that of the SP excitation. Table 2 includes the results of irradiation with various light sources at  $20$  °C. UV irradiation of **1** with a low pressure Hg arc lamp or a pulsed 266-nm laser light produced **2** and **3** in the yield of ca. 50 and ca. 30%, respectively, as mentioned above. In contrast, when a hexane solution of **1** was irradiated with a pulsed 532-nm laser (160 mJ/pulse, 6 ns, 10 Hz) for 1 h, **2** and **3** were obtained in 80 and 13% yields, respectively, with consumption of 20% of **1**. The two-photon nature of the reaction was confirmed by the power dependence of the yields of **2** and **3** (Figure 7), which increased in proportion to the square of the laser intensity. When a CW 514-nm light (2 W) from an Ar<sup>+</sup> laser was used for irradiation, the photoreaction did not occur, even though the integrated intensity for the CW 514-nm light was higher than that of the pulsed 532-nm light, indicating that the photoreaction induced by an intense 532-nm pulsed light is caused by neither heat-up of the sample nor a very weak linear singlet–triplet absorption.

(18) Viscosity data are taken from the following book: Riddick, J. A.; Bunger, W. B.; Sakano, T. K. *Organic Solvents*, 4th ed.; John Wiley: New York, 1986.

(19) Göppert-Mayer, M. *Ann. Physik.* **1931**, *9*, 273.

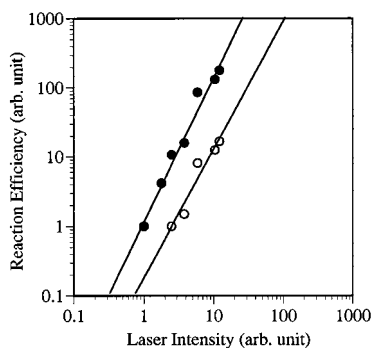


**Figure 7.** Log–log plots of the yields of **2** (●) and **3** (○) vs light intensity under irradiation of **1** with the 532-nm light for 1 h. The laser power was attenuated by using a half-wave plate and a Glan polarizer. The slopes and the correlation coefficients for the linear lines are: 2.1 and 0.977 for **2** and 1.9 and 0.967 for **3**.

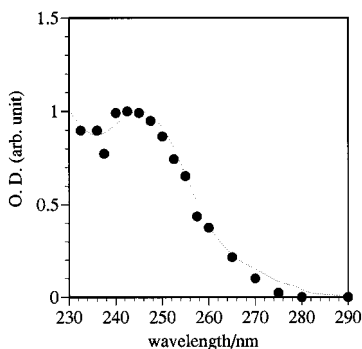


**Figure 8.** Single-photon (dotted line) and two-photon absorption (●) spectra of **1** in hexane. The two-photon spectrum was obtained by plotting the NRTP reaction efficiency against a half of the applied laser wavelength. The maximum of the reaction efficiency was adjusted to the maximum of the single-photon spectrum.

Large effects of solvent polarity were observed also on the NRTP reaction of **1**, as shown in Table 2. Thus, a similar NRTP irradiation of **1** in the presence of 13.4 M of ethanol in hexane gave **2**, **3**, and **4** in 37, 6, and 46% yields, respectively, with 48% conversion, while irradiation with a 266-nm pulsed laser yielded **2**, **3**, and **4** in 33, 23, and 28% yields, respectively; the latter result is in good accord with that of the experiment using a low-pressure Hg lamp (see Table 2). The yields of **2** and **4** during the NRTP irradiation increased in proportion to the square of the laser intensity. Whereas the ratio (2/3) was similar to that in hexane, the solvolytic reaction to give **4** was more favored in the NRTP conditions than in the SP conditions.

Wavelength dependence of the NRTP reaction of **1** was investigated in the range 465–580 nm using laser pulses generated with an optical parametric oscillator (OPO), which was pumped by the third harmonic of a pulsed Nd:YAG laser. Photochemical features similar to those of the NRTP reaction using the 532-nm laser pulses were observed through the wavelength range. Figure 8 shows a plot of the relative efficiency of formation of **2** vs one-half of the wavelength of the incident laser light ( $\lambda_i/2$ ).<sup>12</sup> The reaction efficiency increased with decreasing wavelength from  $\lambda_i = 580$  nm to reach the maximum at  $\lambda_i = 480$  nm. The action spectrum, which should correspond to the two-photon absorption spectrum if the quantum yield of the NRTP reaction is independent on the wavelength, is superimposable to the main feature of the one-photon absorption spectrum of **1** as shown in Figure 8. The polarization ratio ( $\Omega$ ), which is defined as the ratio of the formation efficiency for the circularly polarized light to that

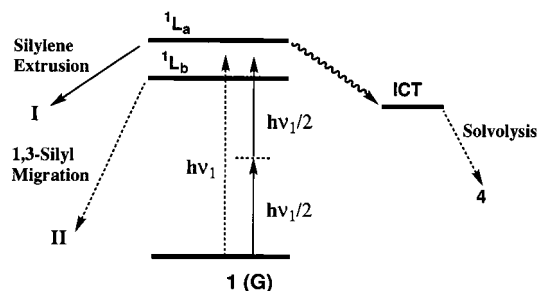


**Figure 9.** Schematic representation of the excited state selection and photoreactions of **1**, depending on the excitation methods.

for the linearly polarized light, was found to be about 0.8 for the NRTP photoreaction of **1**. On the assumption that **1** belongs to  $C_{2v}$  symmetry, the  $\Omega$  value indicates that the overall symmetry of this state is  $A_1$  and that the two-photon allowed excited state is also the one-photon allowed one. Since the allowed absorption band of pentamethylsilyl-substituted benzene at around 230 nm is assigned to  $^1L_a$  with  $A_1$  symmetry, which is strongly coupled with the  $\sigma-\pi$  charge-transfer configuration at the ground-state geometry,<sup>1a,6</sup> the  $^1L_a$  excited state of **1** is also assigned to the lowest  $A_1$  excited state reached by the NRTP excitation.

Since  $^1L_a$  and  $^1L_b$  absorption bands are overlapped in the UV spectrum of **1**, the relative efficiency of  $^1L_a$  to  $^1L_b$  absorptions is difficult to be estimated but may depend on the excitation method; although for both SP and NRTP excitation  $^1L_a$  absorption is allowed and  $^1L_b$  absorption is disallowed, the relative efficiency of  $^1L_a$  and  $^1L_b$  absorptions would be different between SP and NRTP because the  $^1L_b$  absorption may be rigorously forbidden for NRTP. If the NRTP excitation is applied to **1**,  $^1L_a$  state will be generated exclusively, while the SP excitation will give both  $^1L_a$  and  $^1L_b$  state. The present NRTP results may suggest that the silylene extrusion from **1** occurs more preferably through  $^1L_a$  than  $^1L_b$ , while the 1,3-silyl migration occurs through  $^1L_b$  (Figure 9). If the enthalpy difference between the two states is as small as 0.77 kcal/mol as suggested from the temperature dependence on the SP reaction of **1**, facile internal conversion should occur due to the large Franck–Condon factors between the two states, and therefore, no selectivity difference between SP and NRTP reactions will be observed. Instead, it is suggested that the  $^1L_a$  and  $^1L_b$  states are rather far apart in energy and the facile silylene extrusion from  $^1L_a$  state competes with the relaxation from  $^1L_a$  to  $^1L_b$ ; the preferable silylene extrusion for NRTP reaction would be explained by the exclusive formation of the  $^1L_a$  state and the effective silylene extrusion from the state.<sup>20</sup> The temperature dependence on the selectivity found for the SP reaction may be ascribed to a small but significant activation energy for the 1,3-silyl migration from the  $^1L_b$  state. Observed solvent effects on the product distribution for both SP and NRTP reactions suggest that the formation of the ICT state occurs from the  $^1L_a$  state rather than the  $^1L_b$  state in polar solvents.<sup>21</sup>

(20) The authors thank a reviewer for modification of the discussion in this section.

(21) In this relation, it is noteworthy that the efficiency of silylene extrusion from **1** is remarkably dependent on the substituents at the para positions of benzene rings. While the irradiation (LP, 32 W) of a hexane solution of 2,2-di(*p*-tolyl)hexamethyltrisilane ( $9.0 \times 10^{-3}$  M) in the presence of ethanol (1.68 M) gave the ethanol adduct of the corresponding diarylsilylene in 42%, the yields were significantly diminished in the photolysis of 2,2-diphenylhexamethyltrisilane with electron-withdrawing substituents at the para position; the yields were 10 and 0% for 2,2-di(*p*-fluorophenyl)- and 2,2-di(*p*-trifluoromethylphenyl)hexamethyltrisilanes, respectively. The electron-withdrawing substituents may stabilize the ICT state and make the formation of ICT state from  $^1L_a$  state more favorable.

## Concluding Remarks

Several authors have discussed the nature of the excited states responsible for the photochemical silylene extrusion from a trisilane. On the basis of the Woodward–Hoffmann rules, Ramsey concluded that the long wavelength transition is a  $\sigma \rightarrow \sigma^*$  transition and that the reaction occurs from the  $\sigma\sigma^*$  state.<sup>22</sup> A modified correlation diagram was presented using the energy levels calculated by a pseudopotential method.<sup>23</sup> Bock *et al.* have suggested that Rydberg states can play a role in the photochemical silylene extrusion.<sup>24</sup> The potential energy surface of the  $S_1$  state of 2-methyltrisilane has been studied via MC-SCF and multireference MP2 methods.<sup>25</sup>

According to the theoretical calculations of Balaji and Michl,<sup>26</sup> parent trisilane has been shown to have low-lying two-photon allowed excited states; the lowest one is the  $\sigma$ -(SHOMO)– $\sigma$ (LUMO), instead of the  $\sigma$ (HOMO)<sup>2</sup>– $\sigma$ (LUMO)<sup>2</sup> state (doubly excited state), which should be a favorable excited state for the silylene extrusion on the basis of the Woodward–Hoffmann correlation diagram. Our present results suggest that the silylene extrusion occurs through the  $^1L_a$  state of **1**, while the 1,3-silyl migration occurs from the  $^1L_b$  state. Since the  $^1L_a$  state of **1** involves the contribution of the  $\sigma\sigma^*$  state of the Si–Si  $\sigma$  system due to hyperconjugation between the  $\sigma$  (and  $\sigma^*$ ) orbitals and the aromatic  $\pi$  orbitals, the low-lying doubly excited state which is responsible for the silylene extrusion may be produced adiabatically.

## Experimental Section

**General Methods.** <sup>1</sup>H, <sup>13</sup>C, and <sup>29</sup>Si NMR spectra were measured using a Bruker AC-300P (<sup>1</sup>H at 300.1 MHz, <sup>13</sup>C at 75.5 MHz, and <sup>29</sup>Si at 59.6 MHz) and a Varian Unity 300 (<sup>1</sup>H at 299.9 MHz, <sup>13</sup>C at 75.4 MHz, and <sup>29</sup>Si at 59.6 MHz) NMR spectrometers. Electron-impact mass spectra were recorded unless otherwise noted at 70 eV on a JEOL JMS D-300 mass spectrometer. Absorption spectra were recorded on a Milton Roy Spectronic 3000 Array. The product distribution was determined using a Shimadzu GC-14AH capillary gas chromatography.

The fourth harmonic of a pulsed Nd:YAG laser (Spectron Laser Systems, SL803G) was used for excitation at 266 nm (pulse width 4 ns, 10 Hz). The second harmonic of a pulsed Nd:YAG laser (Spectra Physics, GCR 250-10) was used for excitation at 532 nm (pulsed width 6 ns, 10 Hz). The variable-wavelength pulsed lights from 480 to 640 nm, were generated with an optical parametric oscillator (Spectra Physics, MOPO 710), which was pumped by the third harmonic of a pulsed Nd:YAG laser (Spectra Physics, GCR 250-10). The laser intensity of 532- and 266-nm lights was attenuated by using a half-wave plate and a Glan polarizer. A CW Ar<sup>+</sup> laser (Spectra Physics, 2040E) was used for excitation at 514 nm. Linearly and circularly polarized lights were obtained by Soleil-Babinet Compensator.

(22) Ramsey, B. G. *J. Organomet. Chem.* **1974**, *67*, C67.

(23) Halevi, E. A.; Winkelhofer, G.; Meisl, M.; Janoschek, R. *J. Organomet. Chem.* **1985**, *294*, 151.

(24) Bock, H.; Wittel, K.; Veith, M.; Wiberg, N. *J. Am. Chem. Soc.* **1976**, *98*, 109.

(25) Venturini, A.; Vreven, T.; Bernardi, F.; Olivucci, M.; Robb, M. A. *Organometallics* **1995**, *14*, 4953.

(26) Balaji, V.; Michl, J. *Polyhedron* **1991**, *10*, 1265.

**Fluorescence Spectra.** Fluorescence and excitation spectra were recorded on a Hitachi M850 fluorescence spectrometer. The emission and excitation band-pass was fixed to 5 nm. The fluorescence quantum yields were measured by comparing the fluorescence intensities in reference to that for a hexane solution of naphthalene ( $1.48 \times 10^{-5}$  M) at 22–23 °C. All of the samples were thoroughly degassed by freeze–pump–thaw cycles before use.

**Quantum Yields of Photoreactions.** In a typical experiment, several quartz sample tubes containing **1** ( $5.5 \times 10^{-3}$  M) in various ethanol–hexane mixtures together with a sample tube having a cyclopentane solution of 1-phenyl-2-butene ( $2.0 \times 10^{-2}$  M) were irradiated with a low-pressure Hg arc lamp on a Riko rotary photochemical reactor (model RH400-10 W). The light intensity was determined in reference to the progress of the cis–trans isomerization of 1-phenyl-2-butene;<sup>27</sup> the amount of *cis*-1-phenyl-2-butene was corrected for back reaction by Lamola's method.<sup>28</sup> The product yields were determined by means of GLC.

**Solvents.** For photochemical and spectroscopic studies, solvents in spectroscopic grade (Kanto) were purchased. EtOH and CH<sub>2</sub>Cl<sub>2</sub> were distilled over magnesium and calcium hydride, respectively, before use. Hexane was used as such.

**Nonresonant Two-Photon Photoreactions.** In a typical experiment, a quartz cell containing a hexane solution of **1** ( $5 \times 10^{-3}$  M) and ethanol (1 M) was irradiated with 532-nm laser pulses (212 MW/cm<sup>2</sup>) at 20–23 °C. After irradiation for 1 h, the product yields were determined by means of GLC. Products **2** and **3** are characterized in ref 11, and **4** is characterized in this paper.

**Diphenylethoxysilane (2).** A mixture of diphenylchlorosilane (2.3 g, 10.5 mmol), urea (3.7 g, 61.6 mmol), and dry ethanol (2 mL) in dry ether (10 mL) was stirred for 12 h. Extraction with hexane and then Kugelrohr distillation gave **2** in 57.0%. For characterization of **2**, see ref 11.

**Preparative Scale Photoreaction of 1 (Isolation of 3).** Typically, a solution of **1** (50 mg, 0.15 mmol) in a mixture of hexane (10 mL) and ethanol (1 mL) in a quartz tube ( $\varnothing$  10 mm) was deaerated by argon and then irradiated with a spiral low-pressure mercury arc lamp (125 W) for 1 h. After removal of solvents, preparative GLC gave **3** as a colorless oil in the combined yield of 10%. Spectral data for a mixture of two isomers (**A** and **B**, **A/B** = 1/1.4) are described in ref 11.

**Preparative Photoreaction of 1 (Isolation of 4).** Typically, an ethanol (10 mL) solution of **1** (50 mg, 0.15 mmol) in a quartz tube ( $\varnothing$  10 mm) was deaerated by argon and then irradiated with a spiral low-pressure mercury arc lamp (125 W) for 1 h. After removal of solvents, preparative GLC gave **4** as a colorless oil in the isolated yield of 3%. **4**: <sup>1</sup>H NMR (300.1 MHz, CDCl<sub>3</sub>), 7.54–7.51 (m, 4), 7.34–7.32 (m, 6), 4.78 (s, 1), 0.19 (s, 9); <sup>13</sup>C NMR (75.4 MHz, CDCl<sub>3</sub>)  $\delta$  135.7, 134.1, 128.9, 128.0, –1.34; <sup>29</sup>Si NMR (59.6 MHz, CDCl<sub>3</sub>)  $\delta$  –18.2, –31.1; MS *m/z* (relative intensity) 256 (M<sup>+</sup>, 40), 197 (73), 183 (97), 135 (56), 105 (100), 73 (91). HRMS *m/z* (M<sup>+</sup>) Calcd for C<sub>15</sub>H<sub>20</sub>Si<sub>2</sub> 256.1104, found 256.1111.

**Acknowledgment.** This work was supported in part by the Ministry of Education, Science, Sports, and Culture of Japan (Specially Promoted Research No. 02102004 (H.S.) and Grant-in-Aids for Scientific Research (A) No. 08404042 (M.K.)).

JA983370K

(27) Morrison, H.; Peiffer, R. *J. Am. Chem. Soc.* **1968**, *90*, 3428.

(28) Lamola, A. A.; Hammond, G. S. *J. Phys. Chem.* **1965**, *43*, 2129.